3D Catheter Guidance including Shape Sensing for Endovascular Navigation

Sonja Jäckle[a], Verónica García-Vázquez[b], Felix von Haxthausen[b], Tim Eixmann[c], Malte Maria Sieren[d], Hinnerk Schulz-Hildebrandt[c,e,f], Gereon Hüttmann[c,e,f], Floris Ernst[b], Markus Kleemann[g], and Torben Pätz[h]

[a]Fraunhofer MEVIS, Institute for Digital Medicine, Lübeck, Germany
[b]Institute for Robotics and Cognitive Systems, Universität zu Lübeck, Lübeck, Germany
[c]Medizinisches Laserzentrum Lübeck GmbH, Lübeck, Germany
[d]Department for Radiology and Nuclear Medicine, UKSH, Lübeck, Germany
[e]Institute of Biomedical Optics, Universität zu Lübeck, Lübeck, Germany
[f]German Center for Lung Research, DZL, Großhansdorf, Germany
[g]Department of Surgery, UKSH, Lübeck, Germany
[h]Fraunhofer MEVIS, Institute for Digital Medicine, Bremen, Germany

ABSTRACT

Currently, fluoroscopy and conventional digital subtraction angiography are used for imaging guidance in endovascular aortic repair (EVAR) procedures. Drawbacks of these image modalities are X-ray exposure, the usage of contrast agents and the lack of depth information. To overcome these disadvantages, a catheter prototype containing a multicore fiber with fiber Bragg gratings for shape sensing and three electromagnetic (EM) sensors for locating the shape was built in this study. Furthermore, a model for processing the input data from the tracking systems to obtain the located 3D shape of the first 38 cm of the catheter was introduced: A spatial calibration between the optical fiber and each EM sensor was made in a calibration step and used to obtain the located shape of the catheter in subsequent experiments. The evaluation of our shape localization method with the catheter prototype in different shapes resulted in average errors from 0.99 to 2.29 mm and maximum errors from 1.73 to 2.99 mm. The experiments showed that an accurate shape localization with a multicore fiber and three EM sensors is possible, and that this catheter guidance is promising for EVAR procedures. Future work will be focused on the development of catheter guidance based on shape sensing with a multicore fiber, and the orientation and position of less than three EM sensors.

Keywords: catheter guidance, electromagnetic tracking, fiber Bragg gratings, shape sensing, endovascular navigation, endovascular aneurysm repair

1. INTRODUCTION

In western industrial nations cardiovascular diseases like abdominal aortic aneurysm (AAA) are one of the most frequent causes of death.[1] In 80 % of the cases AAAs are free of any symptoms and are usually detected only by chance.[2] However, AAAs with a large diameter have a high risk of rupture, potentially leading to lethal hemorrhages. When AAAs are detected, they can be treated with an endovascular aortic repair (EVAR)

Further author information:
Sonja Jäckle: E-mail: sonja.jaeckle@mevis.fraunhofer.de, Telephone: +49 451 3101 6106

procedure.[3] This procedure is conducted minimal invasive, in which the aneurysm is treated via a stentgraft implantation.

In this minimally invasive procedure, guide wires and catheters guided by fluoroscopy and conventional digital subtraction angiography are used to navigate and fixate the stentgraft. These imaging modalities have several drawbacks. They require the use of X-rays to which both the patient and the physicians are exposed. Furthermore, potentially kidney damaging contrast agent is used to show the current vessel volume.[4] Moreover, fluoroscopy imaging and conventional digital subtraction angiography provide only a two-dimensional projection of the patients anatomy and the medical instruments, which makes the navigation of the guide wires and catheters more difficult, and thus can lead to very long and complex EVAR procedures. Therefore, a 3D catheter guidance based on tracking systems is preferable.

Optical fibers with fiber Bragg gratings (FBGs) are more and more often used for shape sensing of medical instruments.[5–7] FBGs are interference filters inscribed into the core of an optical fiber. They reflect a specific Bragg-wavelength, which is influenced by applied strain and temperature change. Combining multiple FBGs at the same longitudinal position in different fibers or fiber cores results in a FBG array that allows to estimate curvature and direction angle values, which are necessary for shape sensing. In multicore fibers FBG arrays are inscribed in three or more cores of a single optical fiber.[8]

Since optical fibers have a small diameter, are highly flexible and support easy integration into medical instruments with minimal effects on their stiffness, they are perfectly suited for catheter navigation. However, currently they are more frequently used for medical needle shape sensing.[5] When using purely FBG based systems, the information about the position or orientation of the reconstructed shape is missing. For this purpose, electromagnetic (EM) sensors can be used, which can measure the current pose (namely, position and orientation).

EM sensors are one of the most commonly applied techniques for tracking medical tools. As they are very small and thin sensors, they can also be easily integrated into medical instruments.[9] Moreover, in comparison to optical tracking system EM sensors do not require a line of sight to the base station. Several studies have reported the use of EM tracking in bronchoscopy, colonoscopy, radiotherapy, neurosurgery and many other medical fields.[10] In most applications an EM sensor is used to track the position and orientation of medical instruments,[11, 12] which is sufficient in most cases.

To our knowledge no experiments and accuracies of a 3D catheter guidance based on a multicore fiber and EM sensors have been reported in the literature. Shi et al.[13] presented a catheter including an intravascular ultrasound probe, an EM sensor and an optical fiber. However, neither the shape sensing was combined with the EM tracking poses nor accuracies of the shape sensing or of the EM sensors were reported. In this work a novel method including a spatial calibration for determining a located shape based on measurements of a multicore fiber with FBGs and three EM sensors is introduced. The accuracy of this catheter guidance method was evaluated in several 3D experiments.

The remaining part of the paper is organized as follows: First we describe in Section 2.1 the developed catheter prototype and how the shape of the catheter and the EM sensor poses are received from the tracking devices. Section 2.2 details the spatial calibration of the EM sensor system to the fiber optical shape sensing. Using the calibration information, the located 3D shape can be determined with the current tracking data, which is explained afterwards. The whole approach was evaluated in five 3D experiments, which are described in Section 2.3. The resulting accuracies are discussed and compared in Section 3 with previous results reported in literature. The paper ends with Section 4 containing conclusions and future work.

2. MATERIAL AND METHODS

2.1 Catheter prototype

A catheter prototype containing three Aurora Micro 6 degree-of-freedom EM sensors (length: 9 mm, diameter: 0.8 mm; Northern Digital Inc.) placed at the tip, middle and end position of the catheter, and a multicore fiber (FBGS Technologies GmbH) was built, as shown in Fig. 1. The FBG arrays of the multicore fiber are not visible, but a fiber region larger than 38 cm was marked by the manufacturer, where the 38 FBG arrays are located. For
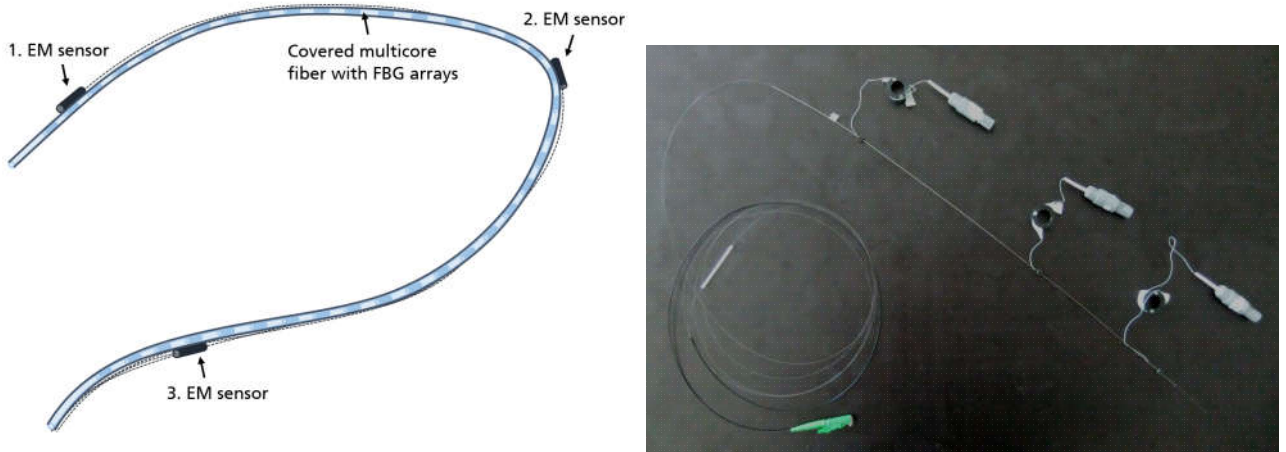
Figure 1. Sketch (left) and picture (right) of the manufactured catheter prototype containing three EM sensors and a covered multicore fiber.

this reason, the EM sensors were placed further inside to be sure that they were in the shape sensing area. The multicore fiber was covered with a metallic capillary tube (400 µm diameter, AISI 304L), which did not interfere with the EM tracking system, to detect the fiber in computed tomography (CT) studies. Each EM sensor was fixed rigidly to the metallic tube with a plastic clip.

2.1.1 Fiber optical shape sensing

The multicore fiber is connected to a fanout and an interrogator (FBGS Technologies GmbH) to receive the reflected wavelength of all FBGs. Based on this input data the shape of 38 cm catheter prototype is reconstructed using the method introduced by Jäckle et al.[14] The resulting shape is represented as a point set

$$\hat{S} = \{S_1, ..., S_n\} \tag{1}$$

of n points. With our fiber of 38 cm length and 20 interpolations per 10 mm we obtain a point set with $n = 760$ points and a distance of $||S_i - S_{i+1}||_2 = 0.5$ mm between adjacent points.

2.1.2 EM tracking

Three EM sensors are tracked with a Tabletop Field Generator (Northern Digital Inc.). The current pose $\hat{P}_k^{EM}$ of each EM sensor $k \in \{1, 2, 3\}$ in the EM space is defined as follows

$$\hat{P}_k^{EM} = \begin{pmatrix} \hat{R}_k^{EM} & \hat{T}_k^{EM} \\ 0 \ \ 0 \ \ 0 & 1 \end{pmatrix} \tag{2}$$

where $\hat{R}_k^{EM}$ is a 3×3 matrix that contains the orientation information and $\hat{T}_k^{EM}$ is a 3-element vector with the position of the EM sensor (specifically, the distal end of the EM sensor).

2.2 Shape localization method

With the EM sensors the poses are measured in the EM space, but in medical applications the position and orientation information in relation to the patients body are needed. Thus EM tracking systems are combined with preoperative computer tomography (CT) scans in several studies.[9,11,12] In this case, markers, which are visible in the CT scan, are placed on the patient for the preoperative scan. During the procedure those markers are placed at the same positions, their positions in the EM space are determined by 'visiting' them with the EM
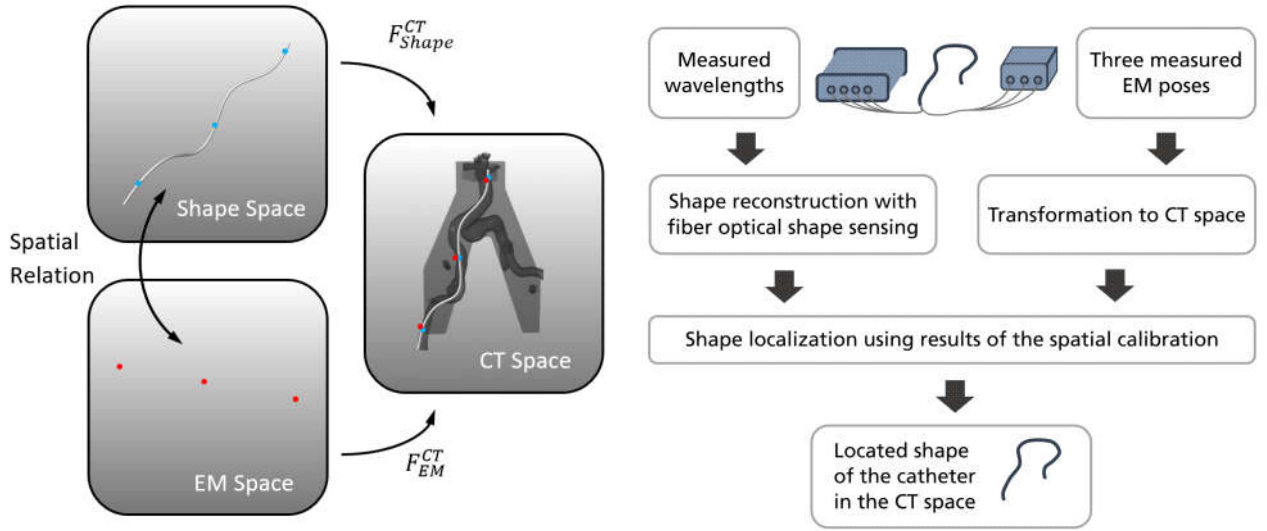
Figure 2. Left: An overview of the different spaces and their relations. Right: Processing pipeline of the catheter guidance method based on the measurements from the multicore fiber and the EM sensors.

sensors. Based on this information a rigid transformation can be computed between the measured marker position and the corresponding position in the CT scan. Using the resulting transformation, the tracking information can be shown in the preoperative CT scan and the physicians can recognize where the catheter is currently located inside the body.

In this work CT studies were made to conduct the spatial calibration step and to evaluate the catheter guidance method. Thus a rigid transformation F_{EM}^{CT}, which transforms the pose of the EM sensors from the EM space $\hat{P}_k^{EM}$ into the CT space

$$\hat{P}_k^{CT} = F_{EM}^{CT} \hat{P}_k^{EM} \tag{3}$$

is determined in every experiment. To determine this transformation m markers are placed in the area of interest in each experiment and their positions

$$M^{EM} = \{M_1^{EM}, \cdots, M_m^{EM}\} \tag{4}$$

in the EM space are measured with the tip of an EM tracked pointer. Afterwards, the positions of the segmented markers

$$M^{CT} = \{M_1^{CT}, \cdots, M_m^{CT}\} \tag{5}$$

in the CT space are obtained. Then, both point sets are used to calculate the rigid transformation F_{EM}^{CT} from the EM space into the CT space by means of point-based registration.[15]

To find a correspondence between the measured shape $\hat{S}$ and the measured pose $\hat{P}_k^{CT}$ of all three EM sensor a spatial calibration is made with a first experiment, as illustrated in Fig. 2 (left). Then, the results of the spatial calibration are used to localize the shape $\hat{S}$ with the positions $\hat{T}_k^{CT}$ of the three EM sensors in each subsequent experiment with the catheter prototype. The processing pipeline of the catheter guidance method is shown in Fig. 2 (right). Each step is now explained in more detail in the following.

2.2.1 Spatial calibration

The catheter was segmented in a CT study and the corresponding shape sensing region S^{CT} was determined manually. After that, the reconstructed shape $\hat{S}$ was aligned to the CT shape of the catheter S^{CT} by means of a point-based registration[15] resulting in $\hat{S}^{CT}$. Afterwards, the position T_k^{CT} of each EM sensor k in the CT scan
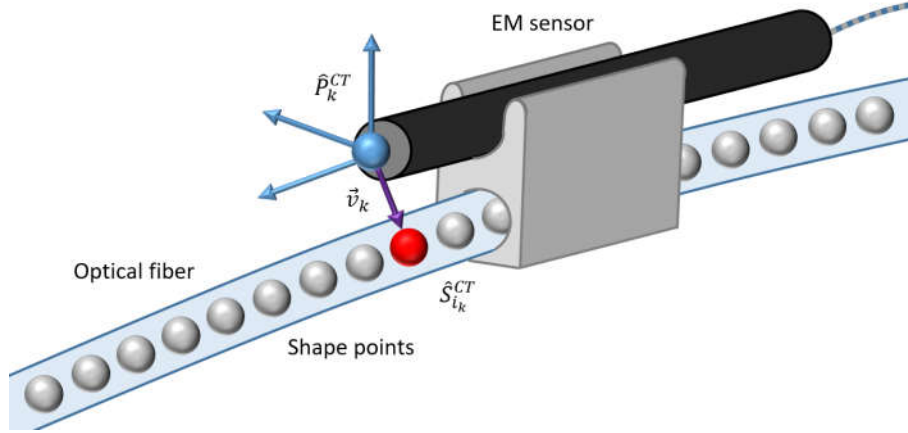
4

Figure 3. An illustration of the calibration step: First the nearest shape point to the distal end of the EM sensor is chosen as corresponding shape point $\hat{S}_{i_k}^{CT}$ (red). Then a correction vector $\vec{v}_k$ (purple) is determined as a function of the EM sensor pose $\hat{P}_k^{CT}$ (blue).

was obtained manually. Then, the index i_k of the nearest shape point $\hat{S}_{i_k}^{CT} \in \hat{S}^{CT}$ to the distal end of each EM sensor position T_k^{CT} was determined, as illustrated in Fig. 3. The shape point with this index was used as the corresponding point for the EM sensor k.

For the second step, a correction vector $\vec{v}_k$ for mapping measured positions $\hat{T}_k^{CT}$ onto their corresponding shape points $\hat{S}_{i_k}$ was calculated for each EM sensor k (see also Fig. 3): It is a linear combination of the EM sensor orientation vectors from the matrix $\hat{R}_k^{CT}$. Its length and direction are the same as those of the translation vector from the CT position of the EM sensor T_k^{CT} to the CT position of the corresponding shape point $S_{i_k}^{CT}$.

After the spatial calibration was done once, the index of the corresponding shape point and the correction vector for each EM sensor were used in subsequent experiments to determine the located shape.

2.2.2 Shape localization with three EM sensors

In each subsequent experiment, the reconstructed shape $\hat{S}$ and the measured poses of the EM sensors $\hat{P}_k^{EM}$ ($k \in \{1, 2, 3\}$) were obtained. Then the shape points in the shape sensing space

$$\{\hat{S}_{i_1}, \hat{S}_{i_2}, \hat{S}_{i_3}\} \tag{6}$$

and the EM sensor positions corrected with the correction vectors in the CT space

$$\{\hat{T}_1^{CT} + \vec{v}_1, \hat{T}_2^{CT} + \vec{v}_2, \hat{T}_3^{CT} + \vec{v}_3\} \tag{7}$$

were determined. Using these two point sets a rigid transformation F_{Shape}^{CT} was determined[15] and used to locate the reconstructed shape $\hat{S}$ in the CT space.

2.3 Evaluation

Five different experiments were done with the catheter prototype. Five metallic markers (The Suremark Company SL10, diameter: 1 mm) were placed at different heights around the catheter prototype to transform the poses of the EM sensors in the CT space. In each experiment, the catheter prototype was fixed in a specific shape to a rigid foam placed on a CT table, as shown in Fig. 4. The data from the optical fiber and the EM sensors were measured before and after acquiring a CT study (which was used to obtain the ground truth) in order to evaluate the stability of the whole setting. Each CT scan was acquired with a Siemens SOMATOM Definition AS+ scanner with the scan parameters: voltage $120\,\mathrm{KVp}$, exposure $97\pm 9\,\mathrm{mAs}$, image size 512 x 512 x 936 and

5

Figure 4. A picture of the 3D curve experiment showing the fixed catheter prototype and the metallic markers. The EM sensors were fixed with double sided tape and surgical tape to ensure no movement of the EM sensors and the optical fiber.

voxel spacing 0.40 x 0.40 x 0.40 mm. The maximal position change c_p and the maximal orientation angle change c_o of the EM sensors before and after each CT acquisition were calculated.

Afterwards, the shape and the EM sensor positions in each CT study were obtained manually and used as ground truth. For the evaluation of the reconstructed shape, the EM sensor positions and the located shape we calculated the average error e_{avg} and the maximum error e_{max} between the calculated positions in the CT space and the corresponding ground truth from the CT study.

3. RESULTS AND DISCUSSION

The results of the different measurements are shown in Tab. 1. The movements of the EM sensors before and after the CT acquisitions were very low, which indicates that the measured poses of the EM sensors should fit to the CT studies, which are used as ground truth.

Accurate shapes ($e_{avg} \leq 0.9\,\mathrm{mm}$ and $e_{max} < 2.3\,\mathrm{mm}$) and EM sensor positions ($e_{avg} < 1.0\,\mathrm{mm}$ and $e_{max} < 1.2\,\mathrm{mm}$) were obtained. The accuracies of the EM sensors were comparable to those shown in previous studies[9,11,12] (specifically for each study, average error: 1.28 mm/1.30 mm/1.20 mm and maximum error: 2.98 mm/1.89 mm/1.70 mm). The errors of the shape reconstruction were higher compared to that presented in[7] (shape reconstruction of a catheter with a length of 11.8 cm, maximum error: 1.05 mm). However, the shape sensing region of our catheter was longer, and the evaluated shapes were more complex and flexible than that shown in.[7] Moreover, the resulting accuracies were comparable to previous experiments with this optical fiber of 38 cm shape sensing length.[14]

The bow experiment was used for the spatial calibration step. Here the corresponding shape points, which had the indices $i_1 = 741, i_2 = 462, i_3 = 64$ and were located at 37.05 cm, 23.10 cm and 3.20 cm along the shape sensing region of the optical fiber, and the correction vectors $\vec{v}_k$ were determined for every EM sensor. When building the catheter prototype, the corresponding shape points were not known exactly because the shape sensing region of the multicore fiber is not visible.

Combining the reconstructed shape obtained from the optical fiber and the measured poses of the EM sensors to obtain the located shape, the average and maximum errors were usually higher than those of the reconstructed shape and the EM sensor positions separately. The reason for this is that both the shape errors and the EM sensor errors affect the accuracy of the located shape. However, the obtained located shapes were still accurate

6

Table 1. Movement of the EM sensors c_p (in mm) and c_o (in degrees) for different shapes, and measured errors e_avg and e_max (in mm) of the reconstructed shape, the EM sensor positions and the located shape.

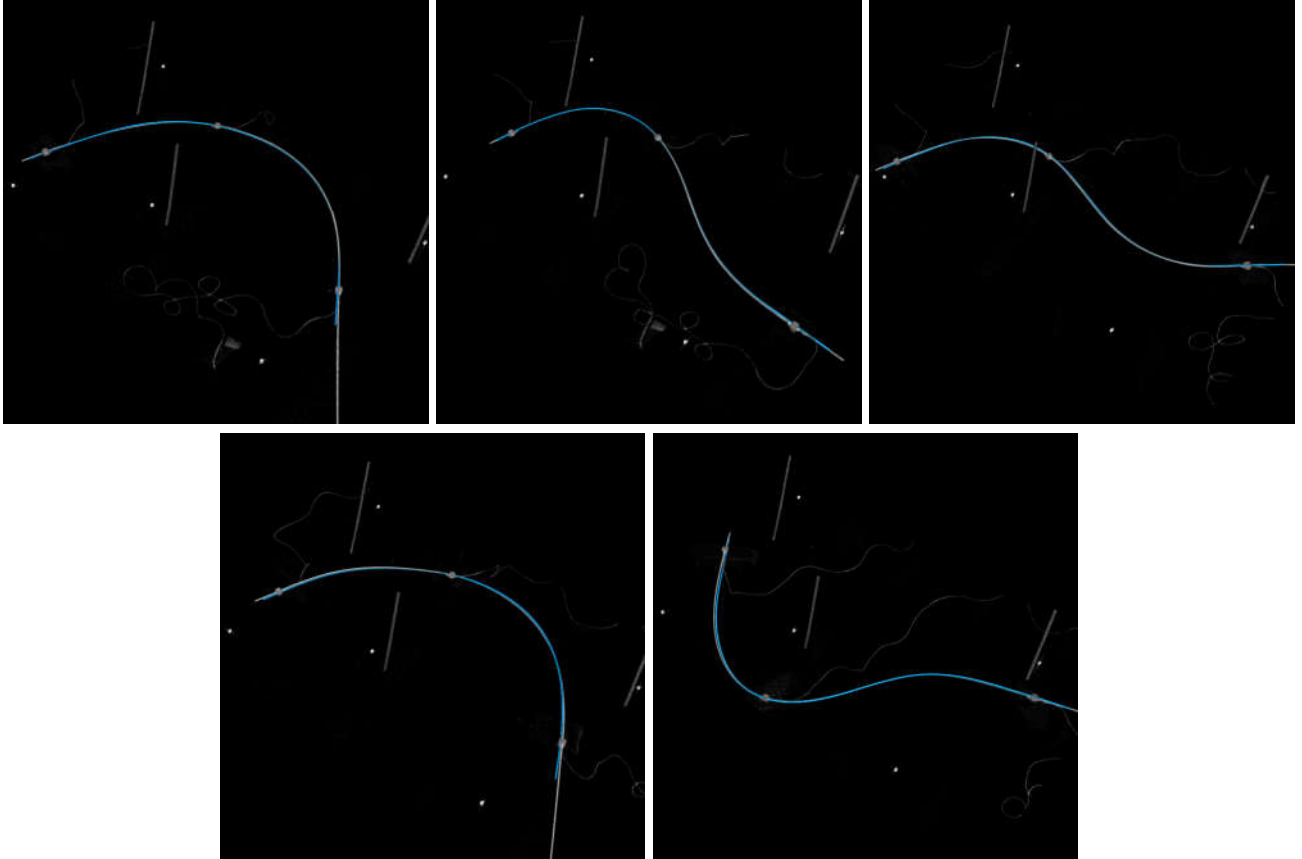|	Movement		Reconstructed shape		EM sensor positions		Located shape	
Shape \ Error	c_p	c_o	e_avg	e_max	e_avg	e_max	e_avg	e_max
Bow	0.04	0.08	0.73	2.19	0.85	0.93	0.99	2.60
Curve	0.10	0.70	0.51	2.05	0.93	0.99	1.10	1.73
S-Curve	0.22	0.26	0.62	2.29	0.65	0.79	1.55	2.45
3D Bow	0.11	0.75	0.90	2.25	0.86	1.12	2.29	2.99
3D Curve	0.04	0.42	0.63	1.01	0.72	0.92	1.15	1.90

Figure 5. CT scans of each experiment with displayed located shapes (blue): Bow, Curve, S-Curve, 3D Bow, 3D Curve (from left to right, from top to bottom).

($e_\mathrm{avg} < 2.3\,\mathrm{mm}$ and $e_\mathrm{max} < 3.0\,\mathrm{mm}$). This is also shown in Fig. 5: The located shapes align closely to the ground truth shapes of the CT scans. The highest shape sensing errors were usually located at the proximal or distal end of the shape (specifically, at the first or last 5 cm of the shape). Thus placing the EM sensors further inside the shape sensing region could lead to better accuracies.

When the EM tracking system will be used in real procedures, higher errors of the EM sensors and thus of the located 3D catheter shapes will be expected. Since these sensors interfere with electronic and metallic objects, the tracking accuracy decreases by medical tools used during the procedures.[10] Another error source is that the metallic markers have to be placed at the same position on the patient for the registration between the EM space and the preoperative CT scan. Further problems are tissue deformation, patient's breathing, arterial

pulsation, and a different patient positioning on the operation table.

Moreover, the fiber optical shape sensing with FBGs has limitations. Shapes with bending diameters less than 2 cm cannot be measured due to the physical properties and the optical fiber can even break. Furthermore, dynamical twist of the catheter during the procedure might not be measured using multicore fibers with parallel arranged FBGs. For this purpose helically wrapped FBGs have been introduced, which can measure the twist of the optical fiber.

4. CONCLUSIONS AND OUTLOOK

In this work, a novel method for a 3D catheter guidance based on tracking systems was introduced. A catheter prototype consisting of a multicore fiber covered with a metallic capillary tube and three EM sensors was built, and a spatial calibration procedure between the shape sensing region of the optical fiber and the EM sensors was described. Based on this determined relation the shape was located by computing a rigid transformation. The shape localization method was evaluated in several experiments.

To our knowledge, no other catheter navigation based on a multicore fiber and EM sensors, which provided an accurate located shape of the first 38 cm of the catheter, has been reported in the literature. Thus, the obtained accuracies of our introduced guidance method are promising for using this approach to navigate catheters in EVAR procedures. In addition, this tracking based solution could also be used in other interventions to enable a 3D guidance of other flexible medical tools, like needles or colonoscopes, to avoid x-ray imaging and the usage of contrast agent.

However, in the described method only the position information of the EM sensors was used to locate the shape of the catheter. Since EM sensors can measure their position and orientation, a shape localization with less EM sensors would be conceivable. Thus future work will focus on reducing the necessary amount of EM sensors for locating the shape, which would even result in a thinner catheter, further expanding areas of application beyond EVAR. Furthermore, our developed 3D catheter guidance method will be evaluated in a more realistic, endovascular setting. For that the optical fiber and the EM sensors will be integrated into a catheter and a 3D printed vessel phantom created from patient data will be used.

ACKNOWLEDGMENTS

REFERENCES

[1] Mendis, S., Puska, P., Norrving, B., et al., [*Global atlas on cardiovascular disease prevention and control*], Geneva: World Health Organization (2011).

[2] Debus, E. S., Kölbel, T., Böckler, D., and Eckstein, H.-H., "Abdominelle Aortenaneurysmen," *Gefässchirurgie* **15**(3), 154–168 (2010).

[3] Cronenwett, J. L. and Johnston, K. W., [*Rutherford's Vascular Surgery*], Elsevier Health Sciences (2014).

[4] Saratzis, A., Melas, N., Mahmood, A., and Sarafidis, P., "Incidence of acute kidney injury (AKI) after endovascular abdominal aortic aneurysm repair (EVAR) and impact on outcome," *European Journal of Vascular and Endovascular Surgery* **49**(5), 534 − 540 (2015).

[5] Shi, C., Luo, X., Qi, P., Li, T., Song, S., Najdovski, Z., Fukuda, T., and Ren, H., "Shape sensing techniques for continuum robots in minimally invasive surgery: a survey," *IEEE Transactions on Biomedical Engineering* **64**(8), 1665–1678 (2017).

[6] Roesthuis, R. J., Kemp, M., van den Dobbelsteen, J. J., and Misra, S., "Three-dimensional needle shape reconstruction using an array of fiber Bragg grating sensors," *IEEE/ASME Transactions on Mechatronics* **19**(4), 1115–1126 (2014).

[7] Khan, F., Denasi, A., Barrera, D., Madrigal, J., Sales, S., and Misra, S., "Multi-core optical fibers with Bragg gratings as shape sensor for flexible medical instruments," *IEEE Sensors Journal* **19**(14), 5878–5884 (2019).

[8] Moore, J. P. and Rogge, M. D., "Shape sensing using multi-core fiber optic cable and parametric curve solutions," *Optics Express* **20**(3), 2967–2973 (2012).

[9] Condino, S., Ferrari, V., Freschi, C., Alberti, A., Berchiolli, R., Mosca, F., and Ferrari, M., "Electromagnetic navigation platform for endovascular surgery: how to develop sensorized catheters and guidewires," *The International Journal of Medical Robotics and Computer Assisted Surgery* **8**(3), 300–310 (2012).

[10] Franz, A. M., Haidegger, T., Birkfellner, W., Cleary, K., Peters, T. M., and Maier-Hein, L., "Electromagnetic tracking in medicine − a review of technology, validation, and applications," *IEEE transactions on medical imaging* **33**(8), 1702–1725 (2014).

[11] de Lambert, A., Esneault, S., Lucas, A., Haigron, P., Cinquin, P., and Magne, J.-L., "Electromagnetic tracking for registration and navigation in endovascular aneurysm repair: a phantom study," *European Journal of Vascular and Endovascular Surgery* **43**(6), 684 − 689 (2012).

[12] Manstad-Hulaas, F., Tangen, G. A., Gruionu, L. G., Aadahl, P., and Hernes, T. A., "Three-dimensional endovascular navigation with electromagnetic tracking: ex vivo and in vivo accuracy," *Journal of Endovascular Therapy* **18**(2), 230–240 (2011).

[13] Shi, C., Giannarou, S., Lee, S.-L., and Yang, G.-Z., "Simultaneous catheter and environment modeling for trans-catheter aortic valve implantation," *International Conference on Intelligent Robots and Systems (IROS 2014)*, 2024–2029, IEEE (2014).

[14] Jäckle, S., Eixmann, T., Schulz-Hildebrandt, H., Hüttmann, G., and Pätz, T., "Fiber optical shape sensing of flexible instruments for endovascular navigation," *International Journal of Computer Assisted Radiology and Surgery* (2019).

[15] Arun, K. S., Huang, T. S., and Blostein, S. D., "Least-squares fitting of two 3-d point sets," *IEEE Transactions on Pattern Analysis and Machine Intelligence* **PAMI-9**(5), 698–700 (1987).